This article has been accepted for publication in a future issue of this journal, but has not been fully edited. Content may change prior to final publication. Citation information: DOI 10.1109/ACCESS.2021.3139223, IEEE Access

IEEE Access
Multidisciplinary | Rapid Review | Open Access Journal

Date of publication xxxx 00, 0000, date of current version xxxx 00, 0000.

Digital Object Identifier 10.1109/ACCESS.2017. Doi Number

Minimally invasive lung tissue differentiation using electrical impedance spectroscopy: a comparison of the 3- and 4-electrode methods

Georgina Company-Se[1], Lexa Nescolarde*[1], Virginia Pajares[2], Alfons Torrego[2], Pere J. Riu[1], Senior Member, IEEE, Javier Rosell[1], Senior Member, IEEE, Ramon Bragós[1]

[1]Department of Electronic Engineering, Universitat Politècnica de Catalunya, Barcelona, 08034 Spain
[2]Department of Respiratory Medicine, Hospital de la Santa Creu i Sant Pau, Barcelona, 08041 Spain

Corresponding author: Lexa Nescolarde (e-mail: lexa.nescolarde@upc.edu).

This work was supported by the Spanish Ministry of Science and Innovation (RTI2018-098116-B-C21/C22) and the Secretariat of Universities and Research of the Generalitat de Catalunya and the European Social Fund

ABSTRACT Multiple imaging techniques are used for the diagnosis of lung diseases. The choice of a technique depends on the suspected diagnosis. Computed tomography (CT) of the thorax and positron emission tomography (PET) are imaging techniques used for the detection, characterization, staging and follow-up of lung cancer, and these techniques use ionizing radiation and are radiologist-dependent. Electrical impedance spectroscopy (EIS) performed through a bronchoscopic process could serve as a minimally invasive non-ionizing method complementary to CT and PET to characterize lung tissue. The aim of this study was to analyse the feasibility and ability of minimally invasive EIS bioimpedance measures to differentiate among healthy lung, bronchial and neoplastic lung tissues through bronchoscopy using the 3- and 4-electrode methods. Tissue differentiation was performed in 13 patients using the 4-electrode method (13 healthy lung, 12 bronchial and 3 neoplastic lung tissues) and the 3-electrode method (9 healthy lung, 10 bronchial and 2 neoplastic lung tissues). One-way analysis of variance (ANOVA) showed a statistically significant difference ($P < 0.001$) between bronchial and healthy lung tissues for both the 3- and 4-electrode methods. The 3-electrode method seemed to differentiate cancer types through changes in the cellular structures of the tissues by both the reactance (Xc) and the resistance (R). Minimally invasive measurements obtained using the 3-electrode method seem to be most suitable for differentiating between healthy and bronchial lung tissues. In the future, EIS using the 3-electrode method could be a method complementary to PET/CT and biopsy in lung pathology diagnosis.

INDEX TERMS bronchi, bronchoscopy, electrical impedance spectroscopy (EIS), electrode methods, lung

I. INTRODUCTION

Respiratory diseases are among the most prevalent illnesses worldwide, along with heart complications. Moreover, each year, an estimated 3 million people die due to respiratory disease complications, making respiratory diseases the third leading cause of death worldwide [1]. Lung cancer is the leading cause of cancer-related death in men and the second-leading cause in women [2]. However, diagnosis in early-stage disease is associated with substantially improved overall survival.

There are different ways to proceed to diagnoses of lung diseases. Computed tomography (CT) allows the detailed representation of interstitial, pleural, mediastinal and vascular structures [4]. Positron emission tomography (PET) provides information about cellular metabolism. Integrated CT with PET (PET/CT) [5] combines the anatomical information from CT with the metabolic information from PET, which makes it possible to obtain a more accurate diagnosis.

Flexible bronchoscopy, the least invasive bronchoscopic procedure, is of limited value for obtaining tissue from lesions in the peripheral segments of the lung.

This work is licensed under a Creative Commons Attribution-NonCommercial-NoDerivatives 4.0 License. For more information, see https://creativecommons.org/licenses/by-nc-nd/4.0/

This article has been accepted for publication in a future issue of this journal, but has not been fully edited. Content may change prior to final publication. Citation information: DOI 10.1109/ACCESS.2021.3139223, IEEE Access

The selection of the biopsy site is relatively simple when the patient has endobronchial involvement. However, in peripheral tumours without endobronchial involvement, additional techniques are necessary to help to confirm that the location of the biopsy is correct. The increasing need to efficiently and safely sample lung lesions has led to the development of virtual bronchoscopy (VB), radial endobronchial ultrasound (r-EBUS), electromagnetic navigation (EMN) and ultrathin bronchoscopes. The diagnostic yield using these bronchoscopic techniques remains suboptimal [6], [7], and their high economic cost makes them unavailable in most centres. To complement the current methods of diagnosing lung diseases, we aim to use electrical impedance spectroscopy (EIS). EIS could allow the differentiation of healthy tissue from tumour tissue and help in the choice of the specific sampling location.

Impedance analysis techniques (such as EIS) consist of the application of electrical current to biological tissues to observe changes in their passive electrical properties [8]. Impedance is the general term used to define the opposition of a conductor to a current flow [9]. When a current is injected into biological tissue, the opposition that biological tissues produce to the current is called bioimpedance. Bioimpedance is composed of two components, resistance (R) and reactance (Xc). On the one hand, the opposition that the physiological fluid, both intracellular and extracellular, presents to a given current flow produces the resistive component. On the other hand, reactance is given by the polarization of the cellular membranes and the tissue interfaces, producing a delay between the current flow and the voltage. This delay defines the parameter called the phase angle (PA) [10], [11]. Both components of bioimpedance (R and Xc) are positively correlated. The current flow applied to the tissues can be either direct current or alternating current. When direct current is applied, the reactive effect disappears, making the bioimpedance completely resistive. This means that when direct current is applied, the current flow circulates only through the physiological fluid. However, when alternating current is applied to tissues, the current is able to flow for both physiological fluid and capacitive elements. This phenomenon makes bioimpedance a frequency-dependent measure [10]. At low frequencies, the current is not able to penetrate the cellular membranes, so there is no conduction within the cells, which is due to the high impedance of the cellular membranes and the tissue interfaces. Therefore, we define the bioimpedance (Z) as a vector as a function of R and Xc [9] and the PA as the arctangent of the ratio between Xc and R.

The impedance modulus (|Z|) is highly correlated with the resistive component, with |Z| being slightly higher than R because of the reactive component [10].

Bioimpedance measures can be obtained using single or multiple frequencies. When the measures are obtained using a single frequency, the most common frequency is 50 kHz due to its high signal-to-noise ratio [10]. Regarding non-invasive single frequency (50 kHz), Toso *et al*. [11] observed a decrease in the Xc parameter and, as a consequence, a decrease in the PA, preserving the R component in patients with lung neoplasms.

Different studies can be found regarding the applicability of EIS for tissue differentiation and characterization [12]–[21]**.** Dean *et al*. [12] and Héroux and Bordages [13] studied the properties of the electrical impedance of biological tissue. They observed changes in impedance as a function of frequency, arriving at the conclusion that the data obtained and the changes in impedance were consistent according to the basic principles of the bioimpedance already introduced. Other studies, such as da Silva *et al*. [14] and Yoon *et al.* [15], investigated the possible use of the technique for the distinction of different types of tissue. The first study was focused on breast tissue and the differentiation between cancerous and healthy tissue. The second study focused on the evaluation of the frequency response of bioimpedance measures in rabbits' tendons through two different types of measures, one longitudinal and other transverse in relation to the tendon fibbers to detect pathological changes in tendons to find the exact location of a tendinitis lesion. Skourou *et al.* [16] and Desai *et al.* [17] evaluated the ability of impedance spectroscopy to detect tumours in their initial stages. The first concluded that the technique allowed the detection of tumours that were not possible to detect with other conventional techniques, such as CT, due to their reduced size. Hillary *et al.* [18] analysed the spectrum of the impedance values obtained for different soft tissues located in the neck, including adipose, parathyroid, thyroid, and muscle tissues. The purpose of the study was to correctly identify the parathyroid tissue to preserve it to facilitate surgery on the parathyroid glands and reduce the occurrence of post-surgery hypoparathyroidism. A bioimpedance method to detect cancer, using a custom-designed catheter with 4-electrodes placed on the front face of a catheter, was tested for Barret's Esophagus [19] and for cervical neoplasia [20].

Regarding the use of EIS to measure lung bioimpedance, Gabriel *et al*. [21] proposed a model to predict dielectric data based on the data present in the literature for different tissues, among which they analysed the inflated lung. Desai *et al*. [17] studied the ability of the technique to differentiate between carcinogenic and healthy cells by extracting different cancer cell types and through pattern recognition techniques evaluating the ability to differentiate between the two types of cells. They studied multiple cancer types, including lung cancer.

Sanchez *et al*. [22], in a previous report, validated the use of minimally invasive EIS with the 4-electrode method for lung bioimpedance measures through a bronchoscopic process. Later, Riu *et al*. [23] published a preliminary report using a single frequency response with a 4-electrode method to differentiate among healthy

This work is licensed under a Creative Commons Attribution-NonCommercial-NoDerivatives 4.0 License. For more information, see https://creativecommons.org/licenses/by-nc-nd/4.0/

This article has been accepted for publication in a future issue of this journal, but has not been fully edited. Content may change prior to final publication. Citation information: DOI 10.1109/ACCESS.2021.3139223, IEEE Access

lung tissue, bronchi and multiple parenchymal pathologies. They found a statistically significant difference with respect to the PA at 33 kHz between healthy lung tissue and bronchial tissue and between bronchial tissue and multiple parenchymal pathologies.
Later more references will be added in the discussion section, to highlight their relationship with our findings.
The use of 4 electrodes in the tip of the catheter produces a local estimation of the tissues in contact with the electrodes and reduces the contribution of electrode-tissue impedances to the measurements; however, we hypothesize that the use of 4 electrodes is more prone to artefacts due to the difficulties in obtaining good contact between all four electrodes and the surrounding tissue. Using the 3-electrode method, only one contact must be established between the catheter and the surrounding tissues. Additionally, the catheter could be simpler, reducing its cost and size. However, there are no previous studies regarding the use of EIS for minimally invasive lung measures for tissue differentiation using the 3- and 4-electrode methods.
The aim of this study was to analyse the capability of minimally invasive EIS, using 3 and 4-electrode methods, to differentiate healthy lung tissue and bronchial and neoplasm lung tissue.

II. MATERIALS AND METHODS

A. PARTICIPANTS

Minimally invasive EIS was performed in 13 patients (69 ± 12 yr; 70.1 ± 15.1 kg; 25.7 ± 4.7 kgm^{-2}) for whom bronchoscopy was indicated during July 2020 at the "Hospital de la Santa Creu i Sant Pau". The bioimpedance measures were obtained via the 4-electrode method (13 healthy lung, 12 bronchial and 3 neoplastic lung tissues) and 3-electrode method (9 healthy lung, 10 bronchial and 2 neoplastic lung tissues).
Ethics approval was obtained from the Hospital de la Santa Creu i Sant Pau (CEIC-73/2010) according to principles of the Declaration of Helsinki for experiments with human beings. All patients provided signed informed consent.

B. MEASUREMENT SYSTEM

To acquire the bioimpedance measures, a tetrapolar catheter, 115 cm long with a diameter of 1.65 mm (5 F), was used (Medtronic 5F RF Marinr steerable catheter with electrode separation 2/5/2 mm) (**Fig. 2**). To convert the 4-electrode measurement system of the catheter to the 3-electrode system, a switch was introduced so that the same catheter could be used for the measures obtained with both three and four electrode methods (**Fig. 1**). Moreover, for the measures obtained with 3 electrodes, two skin electrodes placed on the right side of the patients at the level of the ribs were used (**Fig. 2**).
The measurement system consists of 3 devices (**Fig. 1**): an insulated front end, which is an optically insulated battery-powered patient interface, including the impedance front end; a rugged PC platform based on a PXI system from National Instruments; and an analog–optical interface front end to connect the PXI with the insulated front end. The system includes an arbitrary waveform generator that generates a multisine excitation signal, which is a broadband signal composed of 26 frequencies between 1 kHz and 1 MHz. The front-end includes an AC-coupled current source which ensures a current lower than the maximum allowable patient auxiliary current stablished in the IEC 60601-1:2005 (<1 mA rms measured with the circuit proposed in the IEC 60601-1:2005). The voltage (V(t)) and current (I(t)) are simultaneously acquired. The excitation is converted into an optical signal with the optical–analog interface connected to the PXI. This optical signal is then reconverted into an electrical signal inside the front end. The voltage and current signals, which are optically transmitted from the front end to the optical–electrical interface, are filtered (cut-off frequency 10 MHz) and acquired with the digitizer card. A schematic representation of the bioimpedance acquisition system is shown in **Fig. 1**.
Bioimpedance measures were obtained using the 4-electrode method and the 3-electrode method through bronchoscopy. With the 4-electrodes method, the 4 electrodes located in the distal part of the catheter were placed in the desired area. The external electrodes injected electrical current (high current (HC) and low current (LC)), while the internal electrodes measured the voltage differences generated (high potential (HP) and low potential (LP)). When measuring with three electrodes, the electrode placed at the tip of the catheter was used to inject the current (HC) and to detect the potential (HP), and the LC and LP electrodes were the two skin electrodes placed on the right side of the patient at rib level. A schematic representation of both methods is shown in **Fig. 2**.

C. MEASUREMENT PROTOCOL

To obtain the bioimpedance measures, bronchoscopy, a medical procedure used to inspect the airways, was performed. Prior to bronchoscopy, a radiological imaging technique (CT or PET/CT) was performed as part of the diagnostic process. In addition, the catheter was inserted through a port of the bronchoscope.
During the process, patients were placed in a supine position. The upper airway was anaesthetized with topical 2% lidocaine; intravenous sedation was provided throughout the procedure with midazolam, fentanyl and propofol. All samples were harvested through a flexible bronchoscope during procedures that included endoscopic exploration and other diagnostic tests as required.
Once at the region of interest, measures were taken first with 4 electrodes and then with 3 electrodes after closing the switch (**Fig. 1**). The process was always the same. First, bronchial measures were taken, followed by healthy lung tissue measures and then pathological lung tissue (if any) measures. Once the bronchoscope arrived at the

This work is licensed under a Creative Commons Attribution-NonCommercial-NoDerivatives 4.0 License. For more information, see https://creativecommons.org/licenses/by-nc-nd/4.0/

This article has been accepted for publication in a future issue of this journal, but has not been fully edited. Content may change prior to final publication. Citation information: DOI 10.1109/ACCESS.2021.3139223, IEEE Access

region of interest, we had to ensure that the patient was not moving during the 15 seconds of recording for each location.

D. EIS MEASUREMENTS

Bioimpedance measurements were obtained at the same location with both 4 and 3 electrodes, with approximately 15 seconds of difference between the measurements. EIS consisted on the application of a multisine current signal (26 frequencies from 1 kHz to 1 MHz) and the acquisition of the voltage and current signals. The fast Fourier transform (FFT) was calculated for both the acquired voltage and current signals. The bioimpedance was calculated by obtaining the ratio between the voltage and current coefficients of the FFT corresponding to each injected frequency. 50 spectra per second were acquired along 15 s for each measurement and were averaged to reduce the effect of the modulation induced by ventilation and perfusion.

The 4 electrode configuration measurements were calibrated with 3 saline solutions which covered the measurement impedance range and following the method described in [24]. In the configuration with 3 electrodes, and being two of them in the body surface, this set-up could not be used and was substituted by a measurement over a known resistor (100 Ohms) connected to the catheter tip and to the external electrode connectors.

E. DATA ANALYSIS

In this study, the averaged spectra of the bioimpedance measurements, obtained using the 3 and 4-electrode methods, throughout the acquisition time were used for the tissue differentiation analysis among healthy lung, bronchial and neoplastic lung tissues. The frequency range chosen to visualize the data was 5 kHz – 209 kHz. The values from the frequencies higher and lower than this range were discarded due to electrode and capacitive errors. The interval of 11 kHz – 95 kHz showed a better discriminatory response for tissue differentiation.

For mono-frequency analysis, a central frequency of 33 kHz was chosen (as done in Riu *et al*. [23]) to develop the statistical analysis of |Z|, PA, R and Xc for tissue differentiation between healthy lung tissue and bronchial tissue.

The normality of the distribution of the variables was determined by the Shapiro-Wilk test. Normally distributed variables are shown as the mean ± standard error of the mean (SEM) and 95% confidence interval for the mean (lower limit and upper limit). One-way analysis of variance (ANOVA) was used to determine statistically significant differences in the |Z|, PA, R and Xc values between healthy lung tissue and bronchial tissue for both the 3- and 4-electrode methods.

In the case of the measurements in neoplasic lung tissue, due to the small sample size, the descriptive analysis (for both the 3- and 4-electrode methods) was performed using the mean impedance spectra.

The statistical software IBM® SPSS® version 26.0 (IBM Corp, Armonk, NY, United States) was used for data analysis. The level of statistical significance was set at $P<0.05$.

III. RESULTS

A. MULTI-FREQUENCY RESPONSE FOR MINIMALLY INVASIVE LUNG EIS MEASURES

Fig. 3 and **Fig. 4** show the mean (continuous line) and SD (dashed line) values of |Z|, PA, R and Xc plotted along the frequency range (5 kHz - 209 kHz) used for the measures obtained with 4 and 3-electrode method, respectively. The green line represents healthy lung tissue, the blue line represents bronchial tissue, and the red line represent tissues from three different types of lung neoplasms. The vertical dashed black lines represent the frequency (33 kHz) at which the data were analysed for tissue differentiation.

Table I and **Table II** show the values of |Z|, PA, R and Xc at a frequency of 33 kHz according to measurement location (healthy lung tissue and bronchial tissue) obtained with 4 and 3 electrodes, respectively, in the sample of patients.

B. TISSUE DIFFERENTIATION

Table III lists the descriptive parameters, specified as the mean ± SEM, 95% confidence interval for the mean (lower limit and upper limit), of |Z|, PA, R and Xc and the results of the one-way ANOVA including the Fisher coefficient (F) for the 4-electrode method (healthy tissues: n=13; bronchial tissues: n=12) and the 3-electrode method (healthy tissues: n= 9; bronchial tissues: n=10).

With the use of four electrodes, a statistically significant difference ($P < 0.001$) between healthy tissue and bronchial tissue was observed, with higher Fisher coefficient in Xc ($F=52.103$; $P < 0.001$), |Z| ($F=50.719$; $P < 0.001$) and R ($F=48.648$; $P < 0.001$) and lower Fisher coefficient in PA ($F=30.471$; $P < 0.001$). With the use of 3 electrodes, a statistically significant difference ($P < 0.001$) between healthy tissue and bronchial tissue was also observed, with higher F in |Z| ($F=46.417$; $P < 0.001$), R ($F=46.002$; $P < 0.001$) and PA ($F=43.796$; $P < 0.001$) and lower in Xc ($F=36.784$; $P < 0.001$).

C. LUNG NEOPLASM MEASURES

Fig. 5 and **Fig. 6** show the mean impedance spectra of the values of |Z|, PA, R and Xc plotted along the frequency range (5 kHz - 209 kHz) for the measures obtained from lung neoplasms with 4 and 3 electrodes, respectively; these values could be used to differentiate the different neoplasm types evaluated. The vertical dashed black lines represent the frequency (33 kHz) at which the data were analysed. Each of the colours of the graphs represents a different neoplasm sample. Histologically, lung squamous carcinoma (infiltrating: black and non-infiltrating: red) and lung adenocarcinoma (cyan) were identified. In **Fig.**

This work is licensed under a Creative Commons Attribution-NonCommercial-NoDerivatives 4.0 License. For more information, see https://creativecommons.org/licenses/by-nc-nd/4.0/

This article has been accepted for publication in a future issue of this journal, but has not been fully edited. Content may change prior to final publication. Citation information: DOI 10.1109/ACCESS.2021.3139223, IEEE Access

6, the values obtained from the lung adenocarcinoma (cyan) were discarded due to poor electrode contact because patient coughed.

Table IV shows the values of |Z|, PA, R and Xc obtained at a frequency of 33 kHz from lung neoplasms with both the 4- and 3-electrode methods. In addition, the type of cancer is specified in **Table IV.**

The different cancer types could also be distinguished using only bioimpedance measures, as the measures obtained from different neoplasm types were different from each other, as shown in **Fig. 5** and **Fig. 6.**

Fig. 7 shows the PET/CT images and CT images of each of the lung neoplasm types according to the histological diagnosis.

IV. DISCUSSION

This project, developed by the Universitat Politècnica de Catalunya (UPC) Biomedical Engineering Instrumentation Group and the Interventional Pulmonology Unit of the Respiratory Medicine Department of the Hospital de la Santa Creu i Sant Pau, evaluates the ability of EIS to differentiate lung tissue according to disease state and anatomical location using 3 and 4 electrodes to obtain the measures. The lungs are the organs of the respiratory system, whose most basic function is to facilitate gas exchange [25]. Other structures of the respiratory system are trachea, bronchi, bronchioles. Each of these structures has anatomical and histological characteristics. Therefore, differences in bioimpedance measurement can be expected based on the type of tissue and its state.

This work reports the use of minimally invasive EIS in lungs through a bronchoscopic process using the 4- and 3-electrode methods to differentiate among healthy lung tissue, bronchi and lung neoplasms. A previous study regarding the validation of minimally invasive EIS for lung bioimpedance measures through a bronchoscopic process [22] obtained the measures using the 4-electrode configuration, while the 3-electrode strategy has been used in heart applications [26].

The measured bioimpedance used in this work is proportional to the intrinsic properties of the tissues (conductivity and permittivity) multiplied by a factor, the so called “cell constant” that depends on geometric factors of electrode arrangement and tissue distribution. In order to know the feasibility to differentiate different tissues we used the measured impedance because the application of a cell constant will not modify the comparative results, and also because the cell constant will be unknown for in vivo measurements.

Measures obtained with 4 electrodes reduce the effect of the impedance of the electrode-tissue interfaces. The electrodes are all placed in the distal part of a catheter and are sensitive to the region in contact with the electrodes. In the 3-electrode method, only one electrode is used in the distal tip of the catheter, while the other two electrodes are placed on the skin surface of the thorax [26]. There is an effect on the measured impedance related to the effective area of contact of the electrodes in the catheter against the lung tissue to be investigated. Reducing the contact area will increase the measured impedance due to the increase of current density in the tissue. In the tubular structure of the bronchi and bronchioles the measured impedance will increase if the diameter of the catheter and the diameter of the tubular structure are similar but will decrease as the diameter of the bronchi is bigger and the electrode is losing contact with the tissue surface. Another factor that will modify the measured impedance is the mucosa content (or other liquids for example in the case of carcinoma) in the bronchi or bronchiole. This effect will be higher for healthy tissue because the impedance of the liquid is lower than the impedance of healthy tissue.

The simplest method, the two-electrode method using the tip of the catheter and an external skin electrode, was discarded because the impedance of the skin electrode is also measured and it has high interpatient variability (that is not related to the characteristics of the lung tissue) and depends on skin hydration and sweat regulation.

Other authors [19] [20] have proposed electrode arrangements based on 4 electrodes on the front face of a catheter, either intended to be introduced through an endoscope [19] or to be used as a pencil-like probe [20]. However, these implementations are very thick (3.2 mm and 5.5 mm in diameter) for many in-vivo applications. [27] acknowledged these limitations and developed a probe which is 2 mm in diameter. One of the main problems with all these probes is the very small electrode area (0.5 mm^2, 0.8 mm^2 and 0.2 mm^2 respectively) which increases electrode impedance at low frequencies, up to a point where it is not possible to make measurements due to instrumentation limitations. These limitations are clearly shown in in-vivo measurements [28], where usable data is only at frequencies over 500 kHz, much above the frequency range where we found significant differences in lung tissues. In addition, these probes need to make a perpendicular contact with the tissue, which is not granted in lung tissue at the level of bronchioles.

In contrast, our catheter has only a diameter of 1.67 mm (5F) while keeping electrode areas of about 10 mm^2. Contact can be difficult in the bronchi, but it is granted at the alveolar level. At that level, it would be impossible to make contact with a frontal electrode arrangement without risking breaking the walls of the alveoli.

Other authors, like [29], have proposed more sophisticated arrangements to make measurements in lung tissue in-vivo. However, there are no experimental results with this proposed probe, and to our knowledge, it can also risk damaging the tissue.

Following this description, and due to the trabecular structure of the lung, the placement of the electrodes with

This work is licensed under a Creative Commons Attribution-NonCommercial-NoDerivatives 4.0 License. For more information, see https://creativecommons.org/licenses/by-nc-nd/4.0/

This article has been accepted for publication in a future issue of this journal, but has not been fully edited. Content may change prior to final publication. Citation information: DOI 10.1109/ACCESS.2021.3139223, IEEE Access

the 3-electrode method is easier to perform than with the 4-electrode method (**Fig. 1** and **Fig. 2**) since the 4 electrodes are internal and need to be in contact with the lung tissue. During the bronchoscopy process (used to obtain the bioimpedance measurements of the lungs), patients may cough, despite sedation, and contact between the electrode and the tissue of interest may be lost, resulting in a loss of data.

In this preliminary study the same patient was measured first with 4 electrodes and then with 3 electrodes, increasing the measurements time. Despite sedation, some of them did not tolerate long time without coughing. For this reason, some measurements made with the 3-electrode method had to be removed.

Another aspect taken into account was the possible loss of contact in the two skin surface electrodes in the case of the 3-electrode method (**Fig. 2**). However, this problem did not occur.

In addition, ensuring the contact of the four electrodes in a 4-electrode lateral configuration is not easy and the loss of contact of one of the electrodes may be difficult to detect. Using the described 3-electrode configuration, the loss of contact of one of the electrodes is clearly detected.

The multi-frequency range from 11 kHz to 95 kHz shows a better discriminatory response for tissue differentiation. Healthy lung tissue is clearly differentiable from bronchial and neoplastic lung tissues in both the 4- and 3-electrode methods, while bronchial and neoplastic lung tissues show a similar frequency response.

|Z| and R were higher in healthy lung tissue than in bronchi, while PA and Xc were lower in these locations. Additionally, |Z| and R values obtained with 3 electrodes were higher than those obtained with 4 electrodes. A decrease in the mean PA and Xc values obtained using the 3-electrode method compared with the 4-electrode method was observed. This could be explained because with the 4-electrode method, the voltage drop is sensed at the probe where the current is injected, meaning there are no surrounding tissues that could influence the measure. In contrast, with the 3-electrode method, the voltage drop includes the tissue-electrode impedance of the HC electrode (the distal electrode of the catheter) and the tissues between the catheter and the skin electrodes placed on the right side of the patient (LP) at the level of the ribs, producing an increase in the values of |Z| *and R*. The main contribution to this increment of impedance is due to the tissue-electrode interface because the 3-electrode method shows more sensitivity at the catheter tip due to the decay of sensitivity with the distance to the current injection point [30].

As expected, the |Z| and R values obtained are similar, showing a higher influence of R than Xc on |Z|.

Emphasizing the importance of the analysis of R and Xc according to the theory of Lukaski, Foster and Piccoli [9], [10], [31], [32], we selected the frequency (33 kHz) that allowed us to differentiate among tissues with the 3-electrode method as well as the 4-electrode method, following the preliminary report of Riu *et al*. [23]. According to the results obtained (**Fig. 3** and **Fig. 4**), the optimal frequency could be different from the one analyzed in this work (33 kHz). In the bioimpedance equation ($\boldsymbol{Z = R + jX_c}$), the variable R describes the behaviour of the medium through which the injected current flows, while $\boldsymbol{X_c = -\frac{1}{wC}}$ describes the capacitive component of the cellular membranes [9][10]. The values of modulus Z and PA ($\boldsymbol{|Z| = \sqrt{(R^2 + Xc^2)}}$ and $\boldsymbol{\Phi = \tan^{-1}\left(\frac{Xc}{R}\right)}$, respectively) are dependent on the values of R and Xc. Regarding tissue differentiation at 33 kHz, in both the 4- and the 3-electrode methods, one-way ANOVA reported significant results ($P < 0.001$) for all variables (|Z|, PA, R and Xc). The Fisher coefficient represents the relationship between the inter-group variance and the intra-group variance. Therefore, a higher F coefficient indicates a greater inter-group variance than intra-group variance [33]. For the 4-electrode method, the Fisher coefficient (F) is higher for Xc, while for the 3-electrode method, F is higher for R.

The small number of cancer sample allows only an observational analysis of the medical images obtained by PET/CT, for which the strongest point of CT is the detailed representation of interstitial structures [6]; the confirmation of biopsy sample findings; and the mean impedance spectra of Z|, PA, R and Xc.

The types of cancer analysed (lung squamous carcinoma and lung adenocarcinoma) are included among the non-small-cell lung cancers [34].

The sample sizes of the different cancer types analysed did not allow us to perform a comparative analysis of the cancer histological observations; and the bioimpedance values (|Z|, PA, R and Xc) obtained. Moreover, the small sample size did not allow us to perform a statistical analysis of the measurements obtained with a single frequency at 33 kHz. However, all results seem to indicate that the 3-electrode method seems to differentiate the cancer types in terms of changes in the cellular structures of the tissue (by Xc) as well as in terms of changes in the extracellular fluid-related parameters (R), whereas with the 4-electrode method, only R is able to differentiate between the cancer types. To be able to differentiate using both parameters (R and Xc) with the 4-electrode method, we should increase the frequency at which the bioimpedance samples are analysed; this frequency should be between 70 kHz and 80 kHz.

The mean impedance spectra of the bioimpedance data of the measures obtained with the 4-electrode method and the 3-electrode method show a higher differentiation between cancer samples (black: lung infiltrating squamous carcinoma and red: lung non-infiltrating squamous carcinoma) in the 3-electrode method (|Z| ~ 114.16 **Ω**, PA ~ -3.91º, R ~ 112.83 **Ω** and Xc ~ -20.48 **Ω**) than in the 4-

This work is licensed under a Creative Commons Attribution-NonCommercial-NoDerivatives 4.0 License. For more information, see https://creativecommons.org/licenses/by-nc-nd/4.0/

This article has been accepted for publication in a future issue of this journal, but has not been fully edited. Content may change prior to final publication. Citation information: DOI 10.1109/ACCESS.2021.3139223, IEEE Access

electrode method (|Z| ~ 20.38 Ω, PA ~ 1.01º, R ~ 20.37 Ω and Xc ~ -1.17 Ω), which also seems to indicate that the 3-electrode method is a suitable method to differentiate among cancer types. Although the number of samples in this study is very small, these preliminary observations in neoplastic lung tissue are encouraging for the design of future studies to evaluate the ability of EIS to aid in the selection of biopsy location and thereby the histological characterization of lung diseases.

V. CONCLUSION

In conclusion, the 3- and 4-electrode methods showed a statistically significant difference ($P < 0.001$) to differentiate between bronchial and healthy lung tissues. However. minimally invasive EIS with the 3-electrode method could be more suitable than that with the 4-electrode method because: 1) the 3-electrode method is easier for clinicians to perform because the positioning of the catheter against the tissue is easier; 2) there are fewer motion artefacts in the 3-electrode method; 3) the catheter design could be simpler (only at the distal electrode); and 4) the use of a single electrode in the catheter allows the use of catheters with smaller diameters and increases the extension of the bronchial tree that could be explored.

Regarding to neoplastic tissue, minimally invasive bioimpedance might be able to give information on neoplastic types. These preliminary observations in neoplastic lung tissue are encouraging for the design of future studies to evaluate the ability of EIS to aid in the selection of biopsy location and thereby the histological characterization of lung diseases.

AUTHOR CONTRIBUTIONS

RB, VP, PR, JR, GC, AT and LN designed the experiments; GC, VP and RB performed the experiments; LN, GC and RB performed the data processing; LN, GC and JR analysed the data; GC and LN drafted the manuscript and prepared the tables and figures; and RB, VP, PR, JR, GC, AT and LN revised the paper and approved the final version of the manuscript.

FUNDING

This study was supported by the Spanish Ministry of Science and Innovation (RTI2018-098116-B-C21/C22); the Secretariat of Universities and Research of the Generalitat de Catalunya and the European Social Fund developed in the Electronic and Biomedical Instrumentation Research Group of the Electronic Engineering Department, Universitat Politècnica de Catalunya; and the Interventional Pulmonology Unit of the Respiratory Medicine Department of the Hospital de la Santa Creu I Sant Pau, Barcelona, Spain.

ACKNOWLEDGEMENTS

We would like to especially thank the patients without whom this study would not have been possible. In addition, we would like to thank Laia García Bellmunt, Marta Navarro Colom and Laura Romero Roca from the Interventional Pulmonology Unit of the Respiratory Medicine Department of the Hospital de la Santa Creu i Sant Pau for invaluable support.

REFERENCES

[1] Forum of International Respiratory Societies., *The Global Impact of Respiratory Disease*. 2017.

[2] F. Bray, J. Ferlay, I. Soerjomataram, R. L. Siegel, L. A. Torre, and A. Jemal, "Global cancer statistics 2018: GLOBOCAN estimates of incidence and mortality worldwide for 36 cancers in 185 countries.," *CA. Cancer J. Clin.*, vol. 68, no. 6, pp. 394–424, Nov. 2018, doi: 10.3322/caac.21492.

[3] C. H. Park *et al.*, "Comparative Effectiveness and Safety of Preoperative Lung Localization for Pulmonary Nodules: A Systematic Review and Meta-analysis.," *Chest*, vol. 151, no. 2, pp. 316–328, Feb. 2017, doi: 10.1016/j.chest.2016.09.017.

[4] T. Welte, "Imaging in the Diagnosis of Lung Disease," *Dtsch. Arztebl. Int.*, vol. 111, no. 11, pp. 179–180, 2014, doi: 10.3238/arztebl.2014.0179.

[5] R. Fonti, M. Conson, and S. Del Vecchio, "PET/CT in radiation oncology," *Semin. Oncol.*, vol. 46, no. 3, pp. 202–209, 2019, doi: 10.1053/j.seminoncol.2019.07.001.

[6] D. E. Ost *et al.*, "Diagnostic Yield and Complications of Bronchoscopy for Peripheral Lung Lesions. Results of the AQuIRE Registry.," *Am. J. Respir. Crit. Care Med.*, vol. 193, no. 1, pp. 68–77, Jan. 2016, doi: 10.1164/rccm.201507-1332OC.

[7] J. S. Wang Memoli, P. J. Nietert, and G. A. Silvestri, "Meta-analysis of guided bronchoscopy for the evaluation of the pulmonary nodule.," *Chest*, vol. 142, no. 2, pp. 385–393, Aug. 2012, doi: 10.1378/chest.11-1764.

[8] S. F. Khalil, M. S. Mohktar, and F. Ibrahim, "The theory and fundamentals of bioimpedance analysis in clinical status monitoring and diagnosis of diseases.," *Sensors (Basel).*, vol. 14, no. 6, pp. 10895–10928, Jun. 2014, doi: 10.3390/s140610895.

[9] H. C. Lukaski, "Biological indexes considered in the derivation of the bioelectrical impedance analysis.," *Am. J. Clin. Nutr.*, vol. 64, no. 3 Suppl, pp. 397S-404S, Sep. 1996, doi: 10.1093/ajcn/64.3.397S.

[10] H. C. Lukaski, N. Vega Diaz, A. Talluri, and L. Nescolarde, "Classification of Hydration in Clinical Conditions: Indirect and Direct Approaches Using Bioimpedance.," *Nutrients*, vol. 11, no. 4, Apr. 2019, doi: 10.3390/nu11040809.

[11] S. Toso *et al.*, "Altered tissue electric properties in lung cancer patients as detected by bioelectric impedance vector analysis.," *Nutrition*, vol. 16, no. 2, pp. 120–124, Feb. 2000, doi: 10.1016/s0899-9007(99)00230-0.

This work is licensed under a Creative Commons Attribution-NonCommercial-NoDerivatives 4.0 License. For more information, see https://creativecommons.org/licenses/by-nc-nd/4.0/

This article has been accepted for publication in a future issue of this journal, but has not been fully edited. Content may change prior to final publication. Citation information: DOI 10.1109/ACCESS.2021.3139223, IEEE Access

[12] D. A. Dean, T. Ramanathan, D. Machado, and R. Sundararajan, "Electrical Impedance Spectroscopy Study of Biological Tissues.," *J. Electrostat.*, vol. 66, no. 3–4, pp. 165–177, Mar. 2008, doi: 10.1016/j.elstat.2007.11.005.

[13] P. Héroux and M. Bourdages, "Monitoring living tissues by electrical impedance spectroscopy," *Ann. Biomed. Eng.*, vol. 22, no. 3, pp. 328–337, 1994, doi: 10.1007/BF02368239.

[14] J. Estrela da Silva, J. P. Marques de Sá, and J. Jossinet, "Classification of breast tissue by electrical impedance spectroscopy," *Med. Biol. Eng. Comput.*, vol. 38, no. 1, pp. 26–30, 2000, doi: 10.1007/BF02344684.

[15] K. Yoon *et al.*, "Electrical impedance spectroscopy and diagnosis of tendinitis.," *Physiol. Meas.*, vol. 31, no. 2, pp. 171–182, Feb. 2010, doi: 10.1088/0967-3334/31/2/004.

[16] C. Skourou, P. J. Hoopes, R. R. Strawbridge, and K. D. Paulsen, "Feasibility studies of electrical impedance spectroscopy for early tumor detection in rats.," *Physiol. Meas.*, vol. 25, no. 1, pp. 335–346, Feb. 2004, doi: 10.1088/0967-3334/25/1/037.

[17] S. P. Desai, A. Coston, and A. Berlin, "Micro-Electrical Impedance Spectroscopy and Identification of Patient-Derived, Dissociated Tumor Cells.," *IEEE Trans. Nanobioscience*, vol. 18, no. 3, pp. 369–372, Jul. 2019, doi: 10.1109/TNB.2019.2920743.

[18] S. L. Hillary, B. H. Brown, N. J. Brown, and S. P. Balasubramanian, "Use of Electrical Impedance Spectroscopy for Intraoperative Tissue Differentiation During Thyroid and Parathyroid Surgery.," *World J. Surg.*, vol. 44, no. 2, pp. 479–485, Feb. 2020, doi: 10.1007/s00268-019-05169-7.

[19] C. A. González-Correa *et al.*, "Virtual biopsies in Barrett's esophagus using an impedance probe.," *Ann. N. Y. Acad. Sci.*, vol. 873, pp. 313–321, Apr. 1999, doi: 10.1111/j.1749-6632.1999.tb09479.x.

[20] B. H. Brown, J. A. Tidy, K. Boston, A. D. Blackett, R. H. Smallwood, and F. Sharp, "Relation between tissue structure and imposed electrical current flow in cervical neoplasia.," *Lancet (London, England)*, vol. 355, no. 9207, pp. 892–895, Mar. 2000, doi: 10.1016/S0140-6736(99)09095-9.

[21] C. Gabriel, S. Gabriel, and E. Corthout, "The dielectric properties of biological tissues: III. Parametric models for the dielectric spectrum of tissues," *Phys. Med. Biol.*, vol. 41, no. 11, pp. 2271–2294, 2000, [Online]. Available: http://iopscience.iop.org/article/10.1088/0031-9155/41/11/003/pdf.

[22] B. Sanchez *et al.*, "In vivo electrical bioimpedance characterization of human lung tissue during the bronchoscopy procedure. A feasibility study," *Med. Eng. Phys.*, vol. 35, no. 7, pp. 949–957, 2013, doi: 10.1016/j.medengphy.2012.09.004.

[23] P. J. Riu, G. Company, R. Bragós, J. Rosell, V. Pajares, and A. Torrego, "Minimally Invasive Real-Time Electrical Impedance Spectroscopy Diagnostic Tool for Lung Parenchyma Pathologies*," in *2020 42nd Annual International Conference of the IEEE Engineering in Medicine Biology Society (EMBC)*, 2020, pp. 5077–5080, doi: 10.1109/EMBC44109.2020.9175860.

[24] J.-Z. Bao, C. C. Davis, and R. E. Schmukler, "Impedance spectroscopy of human erythrocytes: system calibration, and nonlinear modeling," *IEEE Trans. Biomed. Eng.*, vol. 40, no. 4, pp. 364–378, 1993, doi: 10.1109/10.222329.

[25] J. F. Murray, "The structure and function of the lung.," *Int. J. Tuberc. lung Dis. Off. J. Int. Union against Tuberc. Lung Dis.*, vol. 14, no. 4, pp. 391–396, Apr. 2010.

[26] G. Amorós-Figueras *et al.*, "Endocardial infarct scar recognition by myocardial electrical impedance is not influenced by changes in cardiac activation sequence," *Hear. Rhythm*, vol. 15, no. 4, pp. 589–596, 2018, doi: 10.1016/j.hrthm.2017.11.031.

[27] A. Keshtkar, "Design and construction of small sized pencil probe to measure bio-impedance," *Med. Eng. Phys.*, vol. 29, pp. 1043–1048, 2007, doi: 10.1016/j.medengphy.2006.10.010.

[28] A. Keshtkar, Z. Salehnia, M. H. Somi, and A. T. Eftekharsadat, "Some early results related to electrical impedance of normal and abnormal gastric tissue.," *Phys. Med.*, vol. 28, no. 1, pp. 19–24, Jan. 2011, doi: 10.1016/j.ejmp.2011.01.002.

[29] R. Baghbani, "Small-sized probe for local measuring electrical properties of the tissues inside of human body: design, modelling and simulation.," *IET nanobiotechnology*, vol. 13, no. 9, pp. 946–951, Dec. 2019, doi: 10.1049/iet-nbt.2019.0040.

[30] M. Ballesta Garcia, "Evaluation of new methods to assess infarcted myocardial tissue by measuring electrical impedance," Polytechnic University of Catalonia (UPC), 2017.

[31] A. Piccoli, B. Rossi, L. Pillon, and G. Bucciante, "A new method for monitoring body fluid variation by bioimpedance analysis: the RXc graph.," *Kidney Int.*, vol. 46, no. 2, pp. 534–539, Aug. 1994, doi: 10.1038/ki.1994.305.

[32] K. R. Foster and H. C. Lukaski, "Whole-body impedance-what does it measure?," *Am. J. Clin. Nutr.*, vol. 64, no. 3 Suppl, pp. 388S-396S, Sep. 1996, doi: 10.1093/ajcn/64.3.388S.

[33] D. F. Morrison, *Multivariate statistical Methods*. 1967.

[34] V. Ambrosini *et al.*, "PET/CT imaging in different types of lung cancer: An overview," *Eur. J. Radiol.*, vol. 81, no. 5, pp. 988–1001, 2012, doi: 10.1016/j.ejrad.2011.03.020.

This work is licensed under a Creative Commons Attribution-NonCommercial-NoDerivatives 4.0 License. For more information, see https://creativecommons.org/licenses/by-nc-nd/4.0/

This article has been accepted for publication in a future issue of this journal, but has not been fully edited. Content may change prior to final publication. Citation information: DOI 10.1109/ACCESS.2021.3139223, IEEE Access

Georgina Company-Se received a B.S. degree in biomedical engineering from the Universitat Politècnica de Catalunya (UPC), Barcelona, Spain, in 2018, and an M.S. degree in computational biomedical engineering from Universitat Pompeu Fabra (UPF), Barcelona, Spain, in 2019. She is currently pursuing a PhD degree in biomedical engineering at UPC. Her research interests include bioimpedance measures and analysis, signal processing and data science. She is interested in machine learning and data science.
Orcid ID: 0000-0002-0473-4955

Lexa Nescolarde was awarded a PhD in biomedical engineering from the Universitat Politècnica de Catalunya (UPC), Barcelona, Spain, in 2006 under the supervision of Professor Javier Rosell. She is currently an associate professor at UPC, and since January 2001, she has been a member of the Electronic and Biomedical Instrumentation Group (IEB) as well as the Centre for Research in Biomedical Engineering (CREB-UPC). Dr Nescolarde's current research interests are focused on the use of non-invasive localized bioimpedance measurement (L-BIA) for muscle assessment in high-performance athletes, body composition analysis and data analysis. Since 2002 and to date, she has participated in 22 research projects and has led 3 research and technology transfer contracts of special relevance, two of which are still valid. Orcid ID: 0000-0001-6861-5106; Scopus Author ID: 6506346116https://futur.upc.edu/LexaDignaNescolardeSelva

Ramon Bragós is an electrical engineer (major in telecommunications engineering, 1991) and has a PhD in electronic engineering (1997) from the Technical University of Catalonia (UPC). Since 1998, he has been an associate professor in the Electronic Engineering Department of UPC. He belongs to the Electronic and Biomedical Instrumentation research group and to the Centre for Research in Biomedical Engineering (CREB). His main area of research is the design of methods and systems for the characterization of biological materials and systems using minimally invasive methods, mainly electrical impedance spectroscopy. Orcid ID: 0000-0002-1373-1588; Scopus Author ID: 6603012697. http://futur.upc.edu/RamonBragosBardia

Virginia Pajares was born in Girona in 1979. She has been a medical doctor and respiratory specialist since 2008. She obtained her PhD in Medicine and Surgery in 2015 from the Universitat Autónoma de Barcelona. Moreover, she is a consultant in the Respiratory Department of Hospital Santa Creu i Sant Pau of Barcelona. She is part of the Bronchosocopy Unit Staff, and she also works as a Respiratory Residents' Mentor. Her main areas of interest are interventional pulmonology, lung cancer and pleural diseases. As of 2021, she is an author of 20 scientific articles in PubMed.

Alfons Torrego was born in Barcelona, Spain, in 1971. He has been a medical doctor and respiratory specialist since 2000 and a consultant in the Respiratory Department of the Hospital Santa Creu i Sant Pau of Barcelona, Spain. He is also the Bronchosocopy Unit Coordinator in Hospital Santa Creu i Sant Pau of Barcelona. Moreover, he is an associate professor of medicine at the Universitat Autònoma de Barcelona and a former chairman of the Spanish Respiratory Society Scientific Committee. His main areas of interest are interventional pulmonology, lung cancer and severe asthma. As of 2021, he is an author of more than 60 scientific articles in PubMed.

Pere J. Riu received an M.Sc. in telecommunication engineering and a PhD in electronic engineering from the Universitat Politecnica de Catalunya (UPC), Barcelona, Spain, in 1986 and 1991, respectively. He is currently a full professor of electronics in the Department of Electronic Engineering, UPC. His research interests include electromagnetic compatibility, computational electromagnetics, the interaction of electromagnetic fields with biological tissues, and biomedical instrumentation design with emphasis on electrical bioimpedance techniques, including electrical impedance tomography (EIT). These activities are performed within the Centre for Research on Biomedical Engineering (CREB, UPC) and the Institut de Recerca Sant Joan de Déu (IRSJD). He was a visiting associate professor in the Department of Bioengineering, University of Pennsylvania, Philadelphia, PA, USA, in 1997. Prof. Riu is currently a senior member of IEEE, a member of the Committee on Man and Radiation (COMAR) (IEEE-BMES), and Vice President of the International Society for Electrical Bio-Impedance.
Orcid ID: 0000-0003-0477-1972
https://futur.upc.edu/PereJoanRiuCosta

Javier Rosell was born in Barcelona, Spain, in June 1959. He received Ingeniero de Telecomunicación and Doctor Ingeniero de Telecomunicación degrees from the Polytechnic University of Catalunya (UPC), Barcelona, Spain, in 1983 and 1989, respectively.
He is currently a Full Professor with the Department of Electronic Engineering, UPC, and head of a research group in the Centre for Research in Biomedical Engineering (CREB-UPC). His current research interest is focused in non-invasive and non-obtrusive measurement methods in sports, medical and biological fields, particularly based on bioelectrical impedance spectroscopy and magnetic induction spectroscopy.
Orcid ID: 0000-0002-9691-328X
https://futur.upc.edu/FranciscoJavierRosellFerrer

This work is licensed under a Creative Commons Attribution-NonCommercial-NoDerivatives 4.0 License. For more information, see https://creativecommons.org/licenses/by-nc-nd/4.0/

This article has been accepted for publication in a future issue of this journal, but has not been fully edited. Content may change prior to final publication. Citation information: DOI 10.1109/ACCESS.2021.3139223, IEEE Access

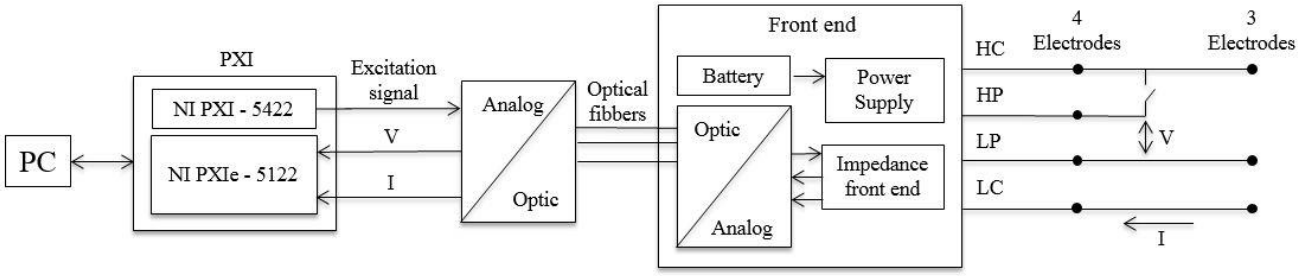

FIGURE 1. **Schematic representation of the bioimpedance acquisition system. For better understanding of the electrodes' connection in each case, please also see Figure 2.**

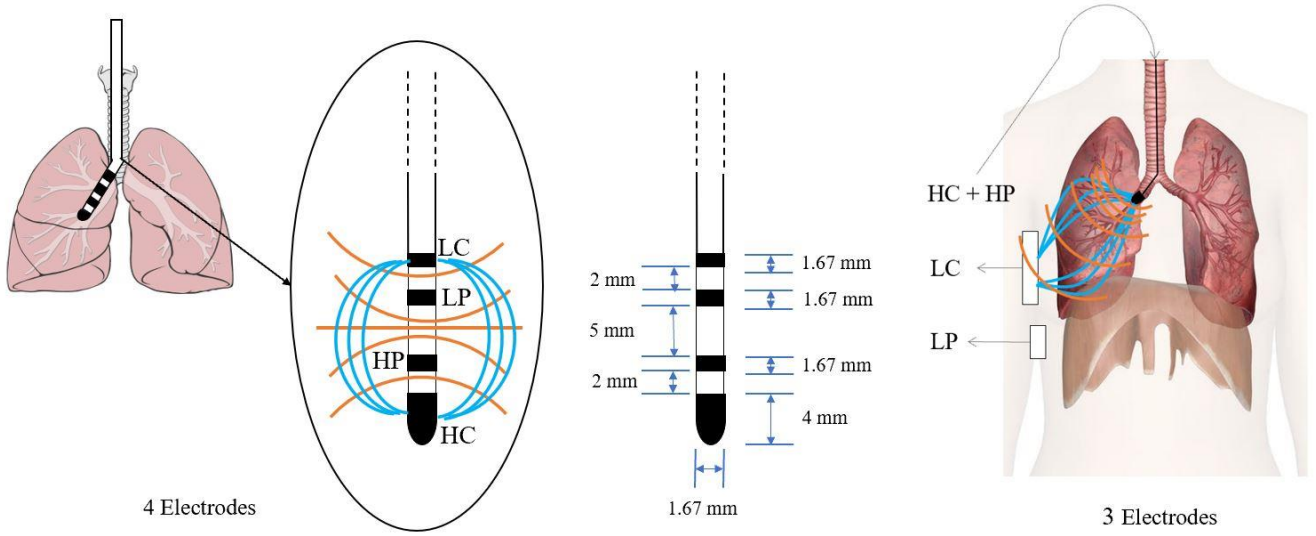

FIGURE 2. **Schematic representation of the 4- (left image) and 3- (right image) electrode methods. Blue lines represent the current lines, and orange lines represent the voltage lines. In 4-electrode method, the four electrode are inside the lung, while 3-electrode method, LC and LP are on the skin using skin surface electrode. In the central figure, the dimensions of the electrodes are represented.**

This work is licensed under a Creative Commons Attribution-NonCommercial-NoDerivatives 4.0 License. For more information, see https://creativecommons.org/licenses/by-nc-nd/4.0/

This article has been accepted for publication in a future issue of this journal, but has not been fully edited. Content may change prior to final publication. Citation information: DOI 10.1109/ACCESS.2021.3139223, IEEE Access

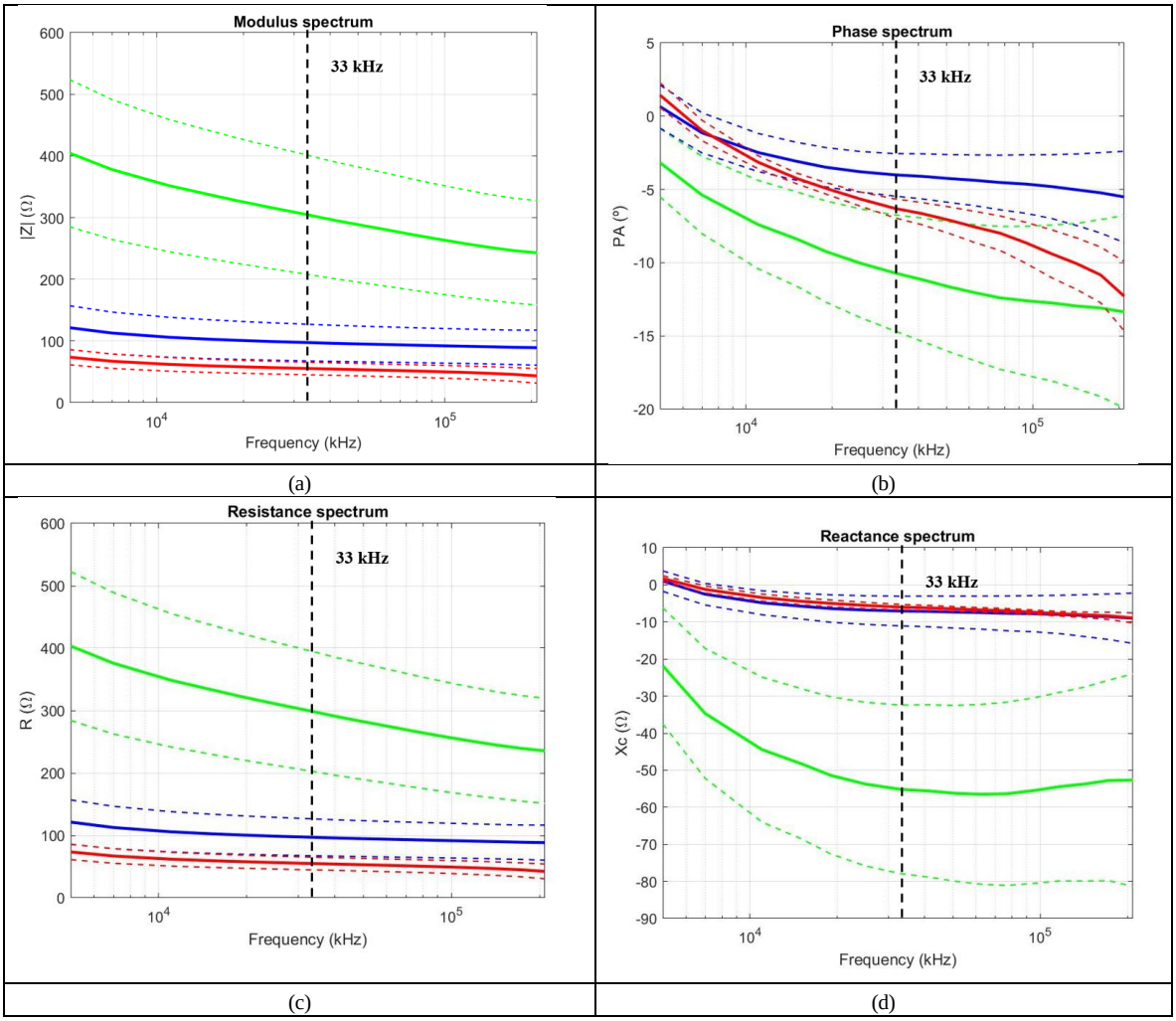

FIGURE 3. The mean (continuous line) and SD (dashed line) values from the bioimpedance signal along the different frequencies analysed obtained with 4-electrode method. The (a) modulus, (b) phase angle, (c) resistance and (d) capacitive reactance. Green: healthy lung tissues; blue: bronchial tissues; red: neoplastic lung tissues.

This work is licensed under a Creative Commons Attribution-NonCommercial-NoDerivatives 4.0 License. For more information, see https://creativecommons.org/licenses/by-nc-nd/4.0/

This article has been accepted for publication in a future issue of this journal, but has not been fully edited. Content may change prior to final publication. Citation information: DOI 10.1109/ACCESS.2021.3139223, IEEE Access

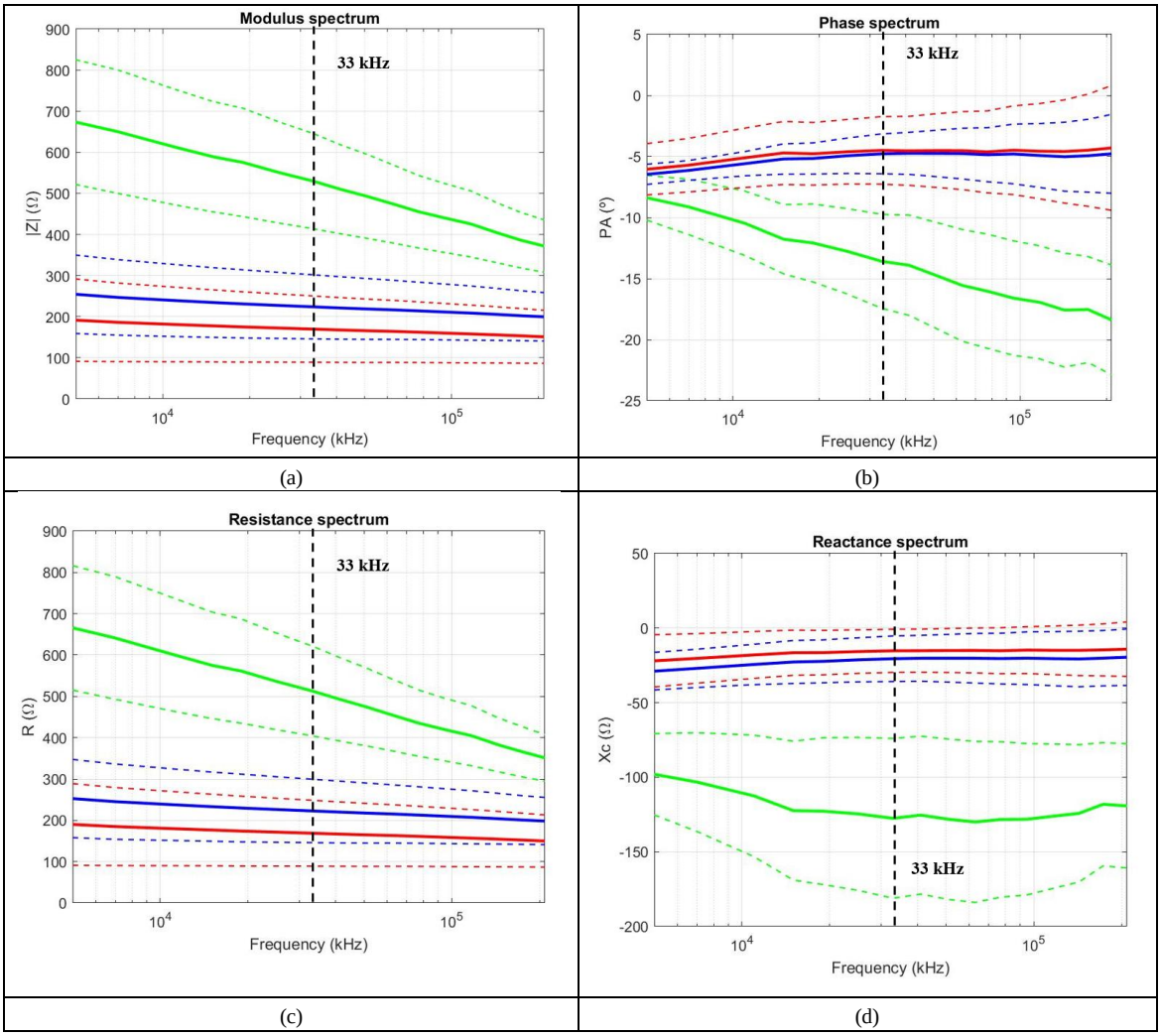

FIGURE 4. The mean (continuous line) and SD (dashed line) values from the bioimpedance signal along the different frequencies analysed obtained with 3-electrode method. The (a) modulus, (b) phase angle, (c) resistance and (d) capacitive reactance. Green: healthy lung tissues; blue: bronchial tissues; red: neoplastic lung tissues.

This work is licensed under a Creative Commons Attribution-NonCommercial-NoDerivatives 4.0 License. For more information, see https://creativecommons.org/licenses/by-nc-nd/4.0/

This article has been accepted for publication in a future issue of this journal, but has not been fully edited. Content may change prior to final publication. Citation information: DOI 10.1109/ACCESS.2021.3139223, IEEE Access

TABLE I

INDIVIDUAL VALUES OF |Z|, PA, R AND XC AT 33 KHZ EXTRACTED FROM THE BIOIMPEDANCE MEASUREMENTS OBTAINED WITH 4 ELECTRODES

Healthy lung tissues					Bronchial tissues				
ID-H	**|Z| (Ω)**	**PA (°)**	**R (Ω)**	**Xc (Ω)**	**ID-B**	**|Z| (Ω)**	**PA (°)**	**R (Ω)**	**Xc (Ω)**
1H-4	215.42	-4.70	214.70	-17.63	**1B-4**	133.77	-3.78	133.48	-8.80
2H-4	257.72	-7.73	255.37	-34.65	**2B-4**	65.92	-4.73	65.70	-5.44
3H-4	359.49	-5.81	357.63	-36.44	**3B-4**	48.61	-2.41	48.57	-2.04
4H-4	249.47	-16.80	238.82	-72.11	**4B-4**	75.03	-2.27	74.97	-2.98
5H-4	421.58	-5.35	419.75	-39.24	**6B-4**	130.09	-7.05	129.11	-15.97
6H-4	507.17	-11.02	497.81	-97.00	**7B-4**	85.32	-5.12	84.98	-7.61
7H-4	135.70	-10.79	133.30	-25.39	**8B-4**	72.06	-4.68	71.82	-5.88
8H-4	258.49	-14.80	249.91	-66.05	**9B-4**	106.02	-3.44	105.83	-6.37
9H-4	344.34	-11.06	337.91	-66.12	**10B-4**	134.78	-5.61	134.13	-13.18
10H-4	283.05	-11.12	277.72	-54.63	**11B-4**	102.12	-3.02	101.98	-5.38
11H-4	380.71	-10.33	374.50	-68.05	**12B-4**	84.69	-3.01	84.57	-4.45
12H-4	250.91	-15.96	241.24	-68.93	**13B-4**	129.74	-2.90	129.58	-6.56
13H-4	301.37	-13.60	292.92	-70.84					

TABLE II

INDIVIDUAL VALUES OF |Z|. PA. R AND XC AT 33 KHZ EXTRACTED FROM THE BIOIMPEDANCE MEASUREMENTS OBTAINED WITH 3 ELECTRODES

Healthy lung tissues					Bronchial tissues				
ID-H	**|Z| (Ω)**	**PA (°)**	**R (Ω)**	**Xc (Ω)**	**ID-B**	**|Z| (Ω)**	**PA (°)**	**R (Ω)**	**Xc (Ω)**
1H-3	429.83	-5.86	427.58	-43.86	**1B-3**	217.89	-4.34	217.26	-16.44
2H-3	607.15	-10.92	596.14	-115.07	**3B-3**	132.55	-3.52	132.29	-8.15
3H-3	585.55	-13.99	568.18	-141.53	**4B-3**	159.61	-3.26	159.35	-9.06
7H-3	372.84	-14.15	361.52	-91.18	**7B-3**	323.93	-7.72	320.99	-43.54
8H-3	634.40	-16.78	607.39	-183.13	**8B-3**	173.34	-3.94	172.93	-11.91
9H-3	668.97	-18.96	632.65	-217.41	**9B-3**	218.43	-4.56	217.73	-17.32
10H-3	629.11	-14.15	610.00	-153.83	**10B-3**	392.00	-7.85	388.32	-53.55
12H-3	400.23	-11.30	392.47	-78.41	**11B-3**	198.67	-4.40	198.09	-15.23
13H-3	443.99	-16.15	426.45	-123.53	**12B-3**	196.00	-3.97	195.53	-13.57
					13B-3	226.28	-4.26	225.66	-16.82

This work is licensed under a Creative Commons Attribution-NonCommercial-NoDerivatives 4.0 License. For more information, see https://creativecommons.org/licenses/by-nc-nd/4.0/

This article has been accepted for publication in a future issue of this journal, but has not been fully edited. Content may change prior to final publication. Citation information: DOI 10.1109/ACCESS.2021.3139223, IEEE Access

TABLE III

DESCRIPTIVE PARAMETERS OF |Z|, PA, R AND XC EXTRACTED FROM THE BIOIMPEDANCE MEASUREMENTS OBTAINED WITH 4 AND 3 ELECTRODES AND ONE-WAY ANOVA TEST RESULTS.

4 Electrodes				
	Mean ± SEM 95% CI (lower limit – upper limit)			
	Healthy tissues (n=13)	Bronchial tissues (n=12)	F	P
|Z| (Ω)	305.34 ± 29.17 (241.14 - 369.53)	97.35 ± 8.60 (78.43 - 116.26)	50.719	0.000
PA (°)	-10.46 ± 1.16 (-13.02 – (-7.89))	-4.00 ± 0.42 (-4.92 – (-3.08))	30.471	0.000
R (Ω)	299.89 ± 29.00 (236.05 - 363.72)	97.06 ± 8.55 (78.24 - 115.88)	48.648	0.000
Xc (Ω)	-53.85 ± 6.70 (-68.61 – (-39.10))	-7.06 ± 1.16 (-9.60 – (-4.51))	52.103	0.000
3 Electrodes				
	Mean ± SEM 95% CI (lower limit – upper limit)			
	Healthy tissues (n=9)	Bronchial tissues (n=10)	F	P
|Z| (Ω)	530.23 ± 38.74 (440.90 - 619.56)	223.60 ± 27.58 (160.00 - 287.21)	46.417	0.000
PA (°)	-13.58 ± 1.28 (-16.54 – (-10.63))	-4.84 ± 0.57 (-6.16 – (-3.52))	43.796	0.000
R (Ω)	513.60 ± 36.30 (429.90 - 597.30)	222.50 ± 27.17 (159.84 - 285.15)	46.002	0.000
Xc (Ω)	-127.55 ± 17.86 (-168.73 – (-86.37))	-20.97 ± 5.38 (-33.37 – (-8.58))	36.784	0.000

This work is licensed under a Creative Commons Attribution-NonCommercial-NoDerivatives 4.0 License. For more information, see https://creativecommons.org/licenses/by-nc-nd/4.0/

This article has been accepted for publication in a future issue of this journal, but has not been fully edited. Content may change prior to final publication. Citation information: DOI 10.1109/ACCESS.2021.3139223, IEEE Access

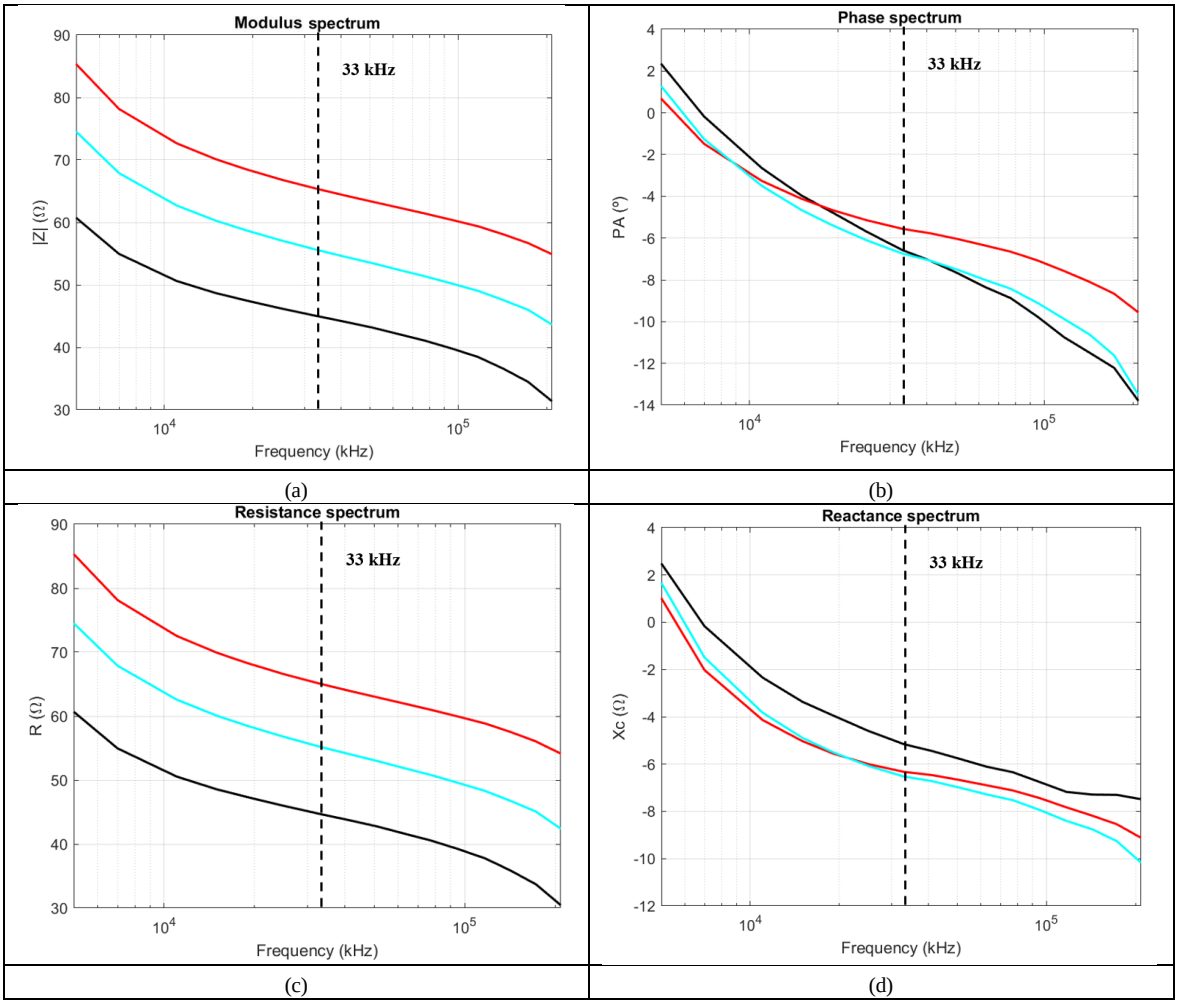

FIGURE 5. Results of the parameters extracted from the bioimpedance signal along the different frequencies analysed obtained with 4 electrodes from lung neoplasms. The a) modulus, b) phase angle, c) resistance and d) reactance of the bioimpedance of all the different measures obtained. Black: lung squamous carcinoma (infiltrating); red: lung squamous carcinoma (non-infiltrating); and cyan: lung adenocarcinoma.

This work is licensed under a Creative Commons Attribution-NonCommercial-NoDerivatives 4.0 License. For more information, see https://creativecommons.org/licenses/by-nc-nd/4.0/

This article has been accepted for publication in a future issue of this journal, but has not been fully edited. Content may change prior to final publication. Citation information: DOI 10.1109/ACCESS.2021.3139223, IEEE Access

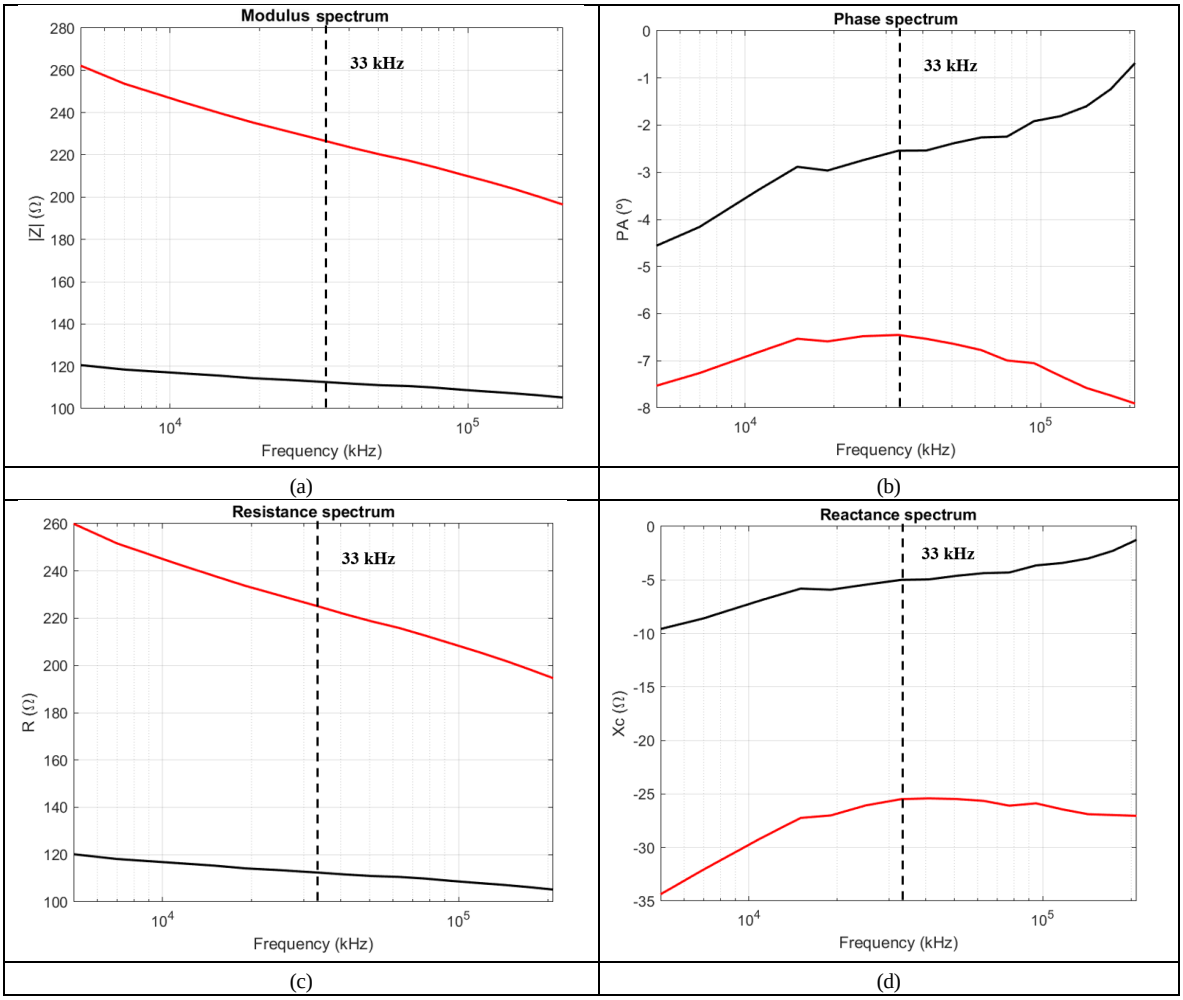

FIGURE 6. Results of the parameters extracted from the bioimpedance signal along the different frequencies analysed obtained with 3 electrodes from lung neoplasms. The a) modulus, b) phase angle, c) resistance and d) reactance of the bioimpedance of all the different measures obtained. Black: lung squamous carcinoma (infiltrating) and red: lung squamous carcinoma (non-infiltrating).

This work is licensed under a Creative Commons Attribution-NonCommercial-NoDerivatives 4.0 License. For more information, see https://creativecommons.org/licenses/by-nc-nd/4.0/

This article has been accepted for publication in a future issue of this journal, but has not been fully edited. Content may change prior to final publication. Citation information: DOI 10.1109/ACCESS.2021.3139223, IEEE Access

TABLE IV
INDIVIDUAL VALUES OF LUNG NEOPLASM MEASUREMENTS OF |Z|, PA, R AND XC EXTRACTED FROM THE BIOIMPEDANCE MEASUREMENTS OBTAINED WITH 4 AND 3 ELECTRODES AND THE CORRESPONDING LUNG NEOPLASM TYPE

Lung neoplasm									
4 Electrodes					3 Electrodes				Cancer type
ID-NL	|Z| (Ω)	PA (°)	R (Ω)	Xc (Ω)	ID-NL	|Z| (Ω)	PA (°)	R (Ω)	Xc (Ω)	
1NL-4	45.00	-6.57	44.70	-5.16	**1NL-3**	112.55	-2.54	112.44	-5.00	Lung squamous carcinoma (infiltrating)
4NL-4	65.38	-5.56	65.07	-6.33	**4NL-3**	226.71	-6.45	225.27	-25.48	Lung squamous carcinoma (non-infiltrating)
5NL-4	55.60	-6.74	55.22	-6.52						Lung adenocarcinoma

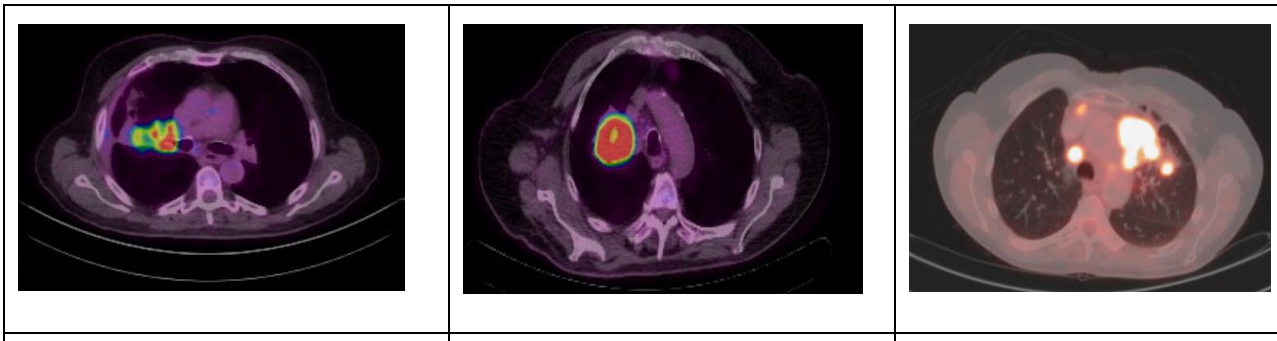

(a) (b) (c)

FIGURE 7. PET/TC and CT images of the lung neoplasms. The histological diagnoses were a) lung squamous carcinoma (infiltrating), b) lung squamous carcinoma (non-infiltrating) and c) lung adenocarcinoma.

This work is licensed under a Creative Commons Attribution-NonCommercial-NoDerivatives 4.0 License. For more information, see https://creativecommons.org/licenses/by-nc-nd/4.0/